中国激光

高功率高光束质量全固态内腔三倍频355 nm激光器

刘鑫宇[1]，张艳林[1]，曹雪辰[1]，杨婕[1]，苏静[1,2]，卢华东[1,2*]

[1]山西大学光电研究所量子光学与光量子器件国家重点实验室，山西 太原 030006；

[2]山西大学极端光学协同创新中心，山西 太原 030006

摘要 通过设计优化二倍频晶体的参数，较好地补偿了基频光与倍频光在三倍频晶体中混频时产生的走离效应。通过设计优化谐振腔参数，增大了三倍频晶体处基频光束的光斑半径，使穿过三倍频晶体的基频光束接近平行，从而减小了三倍频晶体处基频光束的发散角，进一步提高了三倍频转换效率。当泵浦注入功率为96.8 W，脉冲重复频率为35 kHz时，355 nm紫外激光的平均输出功率最高为14.1 W，10 h的功率稳定性（均方根）优于0.9%，光束质量因子优于1.18。整个系统具有结构简单、平均功率高、功率稳定性高、光束质量好等优点，适合进行产品化开发。

关键词 355 nm紫外激光器；腔内三倍频；走离补偿；高功率；全固态

中图分类号 TN248 **文献标志码** A **DOI**：10.3788/CJL240477

1 引 言

高功率、高光束质量的全固态355 nm紫外（UV）激光器因其具有短波长、易聚焦、高能量等特点，已经广泛应用于精细加工、生物医学、光学制造、光学传感等领域[1-5]。最常用的实现355 nm紫外光输出的技术手段是使用主振荡功率放大器（MOPA）系统，该系统首先对1064 nm的种子光进行单级或多级放大，然后在腔外通过三倍频频率变换来获得所需的紫外光。2010年，Yan等[6]采用由Nd∶YVO_4组成的MOPA对种子源进行功率放大，然后通过级联二倍频和三倍频过程，获得了35.1 W的355 nm紫外激光输出，泵浦光到紫外光的光-光转换效率为13%。为了提高三倍频过程中的转换效率，2013年，Chen等[7]利用单频1064 nm激光器作为种子光源，通过光纤MOPA和固体MOPA，实现了43.7 W的355 nm紫外激光输出，泵浦光到紫外光的光-光转换效率提高到18.2%。尽管采用MOPA对基频光进行单级或多级放大，再通过腔外三倍频技术可以保证355 nm紫外激光的高功率输出，但是系统整体相对复杂，不利于获得高稳定的紫外激光。另外，为了提高三倍频过程中的转换效率，通常会缩小基频光和倍频光在三倍频晶体处的腰斑尺寸以提高二者的功率密度，由此导致三倍频晶体端面的镀膜涂层在高功率密度激光长时间照射下极易损伤。

与腔外三倍频技术相比，腔内三倍频技术不仅可以充分利用腔内基频光功率密度高的优点，而且激光器整体结构紧凑、稳定性高，是实现高功率高稳定性全固态355 nm紫外激光器的有效手段之一[8]。同时，为了延长三倍频晶体的使用寿命，研究者采用布儒斯特角切割的三硼酸锂（LBO）晶体作为腔内三倍频频率变换的非线性介质。但是布儒斯特角的引入会导致基频光产生像散，进而影响355 nm输出光束质量和转换效率。因此，2019年，Yang等[9]设计了凸凹镜相结合的谐振腔结构，有效补偿了布儒斯特角切割的LBO晶体引入的像散，获得了3.65 W的355 nm紫外激光输出，横向光束质量因子（M_x^2）和纵向光束质量因子（M_y^2）分别为1.32和1.14。2023年，Xu等[10]利用一种由平凸镜构成的折叠谐振腔结构，通过采用级联LBO晶体实现了频率变换，获得了12.2 W的355 nm紫外激光输出。尽管该工作通过使用凸面入射镜优化了谐振腔的工作稳区，但是由于三倍频晶体采用端面为布儒斯特角切割的LBO晶体，其输出的355 nm紫外激光的M_x^2和M_y^2分别为1.18和1.24。为了获得高功率高光束质量的355 nm紫外激光输出，我们设计了四镜折叠腔结构，通过使用可实现走离补偿的腔内级联非线性LBO晶体，提高了355 nm紫外激光的输出功率和转换效率，获得的355 nm紫外激光的光束质量因子优于1.18。

收稿日期：2024-01-10；**修回日期**：2024-01-28；**录用日期**：2024-02-21；**网络首发日期**：2024-03-13

基金项目：国家自然科学基金（61975100，62105192）、国家重点研发计划（2022YFC2204003）、山西省杰出青年培育项目（202103021221004）、山西省留学基金委资助研究项目（2022-015）、山西省科技创新人才计划（202204051002005）、山西省专利转化专项计划（202305007）、山西省1331工程项目、第一实验室-国创中心（山西）科技创新项目

通信作者：*luhuadong@sxu.edu.cn

2 实验装置

实现高功率高光束质量355 nm紫外激光输出的实验装置如图1(a)所示。泵浦源采用光纤耦合输出的中心波长为888 nm的半导体激光二极管(LD),其最大平均输出功率为120 W,光纤芯径为400 μm,数值孔径为0.22。增益介质采用a轴切割的掺杂物原子数分数为0.8%的Nd:YVO_4单端键合晶体,尺寸为3 mm×3 mm×(3+20) mm,掺杂部分长度为20 mm,未掺杂部分长度为3 mm,双端面均镀有1064 nm与888 nm减反膜,整个Nd:YVO_4晶体被置于循环冷却水中进行水冷散热。为了实现泵浦光和激光谐振腔之间的模式匹配,在激光谐振腔前面放置泵浦耦合系统,该泵浦耦合系统由焦距分别为f_1=30 mm和f_2=100 mm的凸透镜组成,使得泵浦光准直聚焦在Nd:YVO_4晶体上。激光谐振腔由2个平凸镜(M_2和M_3)和2个平面镜(M_1和M_4)组成。其中:输入镜M_2是曲率半径为R=500 mm的平凸镜,折叠镜M_3是曲率半径为R=1000 mm的平凸镜,二者的凸面均镀有1064 nm高反膜和888 nm减反膜,平面镀有888 nm减反膜,入射角为10°;腔镜M_1为镀有1064 nm高反膜的平面镜;腔镜M_4则镀有1064 nm与532 nm双高反膜。腔内插入的M_5一面镀有532 nm和355 nm高反膜及1064 nm减反膜,另一面镀有1064 nm减反膜,利用该镜子可以将产生的355 nm紫外激光从腔内输出到腔外。M_6为镀有888 nm高反膜的平面镜,单次穿过增益晶体而未被吸收的泵浦光经M_6反射,再经过焦距为f_3=100 mm的凸透镜聚焦返回到Nd:YVO_4晶体中,从而提高888 nm到1064 nm激光的光-光转换效率。在考虑腔内增益晶体热透镜效应[11]的基础上,通过计算得到四镜"Z"形谐振腔内各处光斑半径的变化图,如图1(b)所示。通过对M_2、M_3曲率半径的选取实现了谐振腔两臂处不同光斑大小分布。在总腔长为563 mm的条件下,Nd:YVO_4晶体处的光斑半径ω_1为533 μm,靠近端镜M_1处的光斑半径ω_3为374 μm,靠近端镜M_4处的光斑半径ω_2为418 μm。为了提升声光Q开关的关断效果,将声光晶体放置在腰斑较小的M_1端镜处。为了降低LBO晶体的热效应以保证腔内谐波在高功率工作时的高光束质量输出,将LBO晶体放置在腰斑较大的M_4端镜处。同时从图1(b)还可以看出,LBO晶体所在光路的基频光束接近准直状态。在实验中,基频光为水平线偏振光,当两块LBO晶体分别为I、II类角度匹配的非线性晶体时,基频光通过I类角度匹配的LBO晶体后,产生的二次谐波是与基频光偏振态垂直的竖直偏振光,入射的基频光和产生的倍频光恰好满足三倍频LBO晶体的II类角度相位匹配条件,从而实

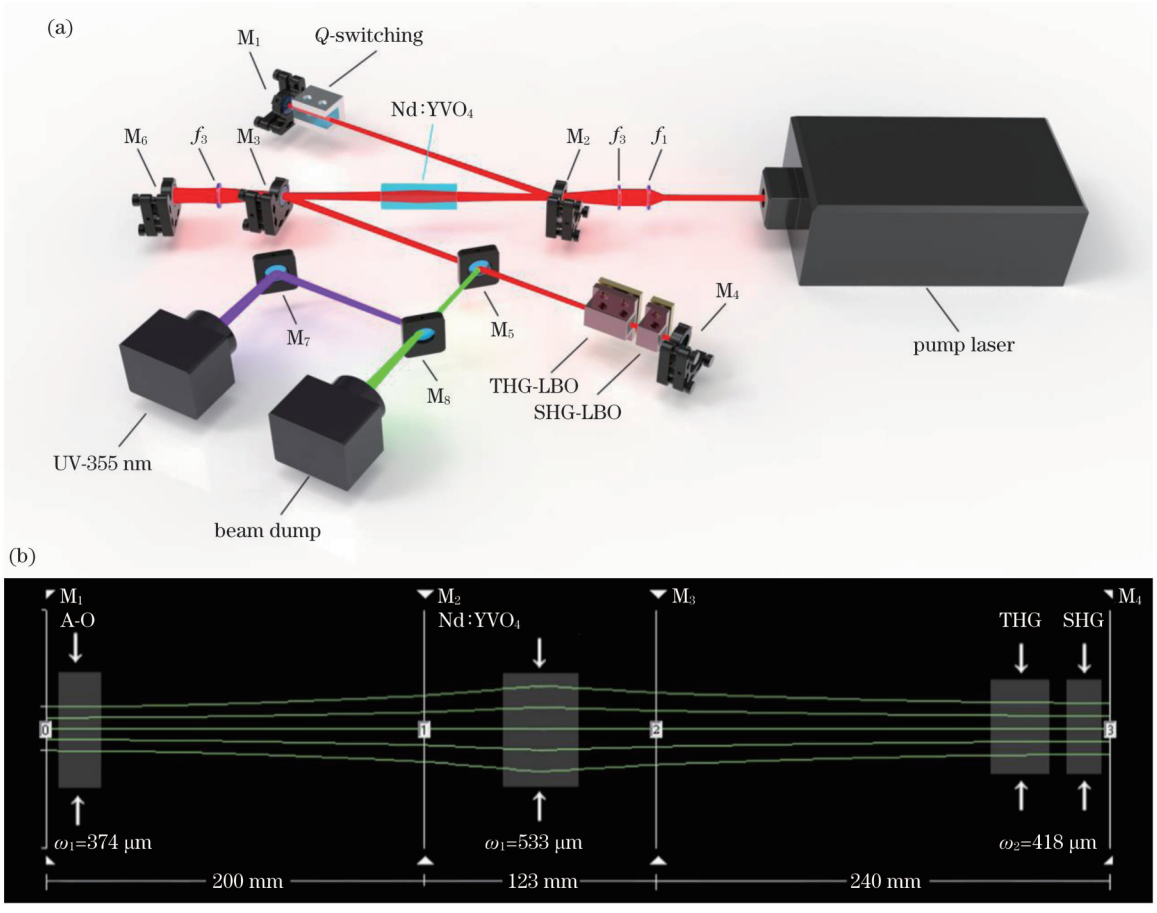

图1 实验装置和光斑尺寸。(a)实验装置示意图;(b)谐振腔内光斑尺寸分布

Fig. 1 Experimental setup and spot size. (a) Schematic of experimental setup; (b) spot size distribution in resonant cavity

现三倍频 355 nm 紫外激光输出[12-15]。为了有效减小产生的 532 nm 和 355 nm 激光对腔内其他光学元件尤其是增益晶体的影响，在谐振腔内插入镀有 532 nm 与 355 nm 双高反膜以及 1064 nm 高透膜的分光镜 M_5，谐振腔产生的 355 nm 和 532 nm 激光由 M_5 输出，然后通过 M_7、M_8 两个分光镜将出射光中残留的少量 1064 nm 基频光和 532 nm 绿光滤除，并利用功率计对 355 nm 紫外光输出功率及其长期稳定性进行监测。

3　结果与分析

在进行非线性频率变换时，非线性晶体的相位匹配方式及参数设计是影响三倍频过程（THG）中转换效率和输出激光光束质量的关键。当 1064 nm 基频光经过角度匹配的二倍频 LBO 晶体时，角度匹配使得基频光和倍频光在 xy 平面内产生走离[16-18]，而当基频光和倍频光通过 II 类角度匹配的三倍频 LBO 晶体时，则倍频光与基频光在 yz 平面内产生走离。这时，如果两块 LBO 晶体的光轴方向一致，两束光首先在二倍频过程（SHG）中发生走离现象，然后在三倍频过程中发生走离现象，二者叠加导致三倍频晶体内绿光与基频光的交叠区大幅度减小，从而使得三倍频过程中的转换效率下降，如图 2(a)所示。当两块 LBO 晶体的光轴方向不一致时，在二倍频晶体中走离导致分开的基频光和倍频光则在经过三倍频晶体后又重合到一起，使得两束光在三倍频晶体中的交叠区域变大，最终可以获得高功率和高转换效率的 355 nm 紫外激光输出，如图 2(b)所示。图 2(a)、(b)中 xyz 和 $x'y'z'$ 坐标系表示两块晶体的主轴坐标系。

利用文献[19-24]中二倍频转换效率的计算结果，并结合谐振腔设计对非线性晶体处的腔模进行计算，得出二倍频 LBO 晶体的长度（L_{SHG}）为 12 mm，三倍频 LBO 晶体的长度（L_{THG}）为 19 mm，晶体的横截面尺寸均为 3 mm×3 mm。其中：二倍频 LBO 晶体的相位匹配角为 $\theta=90°$，$\Phi=11.2°$，两端面均镀有 1064 nm 与 532 nm 减反膜；三倍频 LBO 晶体的相位匹配角为 $\theta=42.2°$，$\Phi=90°$，两端面均镀有 1064、532 与 355 nm 减反膜。当重复频率为 35 kHz 时，所获得的 355 nm 紫外激光输出功率曲线如图 3(a)所示。可以看出：当两块非线性晶体的走离叠加时，激光器的功率阈值为 76.6 W，当最大泵浦功率为 96.8 W 时，获得的 355 nm 紫外激光的最大输出功率为 11.4 W，此时的光-光转换效率为 11.7%；当两块非线性晶体的走离得到补偿时，激光器的功率阈值不会发生变化，仍然为 76.6 W，355 nm 紫外激光的最大输出功率则提升到 12.1 W，光-光转换效率则提高到 12.5%。实验结果表明，当两块非线性晶体的走离得到有效补偿时，激光器的输出功率和转换效率均会得到一定提升。为了进一步提高 355 nm 紫外激光的输出功率，我们在实验上通过改变倍频晶体长度来优化两块晶体之间的走离补偿。图 3(b)表示的就是倍频晶体长度分别为 10、11 和 12 mm 时，355 nm 紫外激光的输出功率曲线。可以看出，当二倍频晶体长度为 11 mm 时，355 nm 紫外光平均输出功率达到最

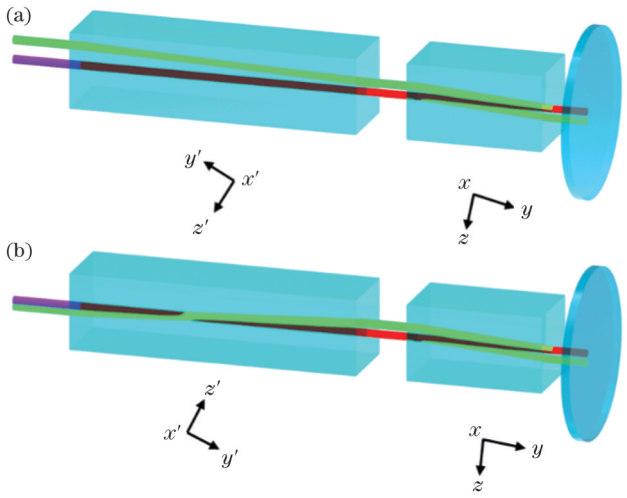

图 2　光束空间走离原理示意图。(a)未补偿；(b)补偿

Fig. 2　Schematics of beam spatial walk-off principle. (a) Uncompensated case; (b) compensated case

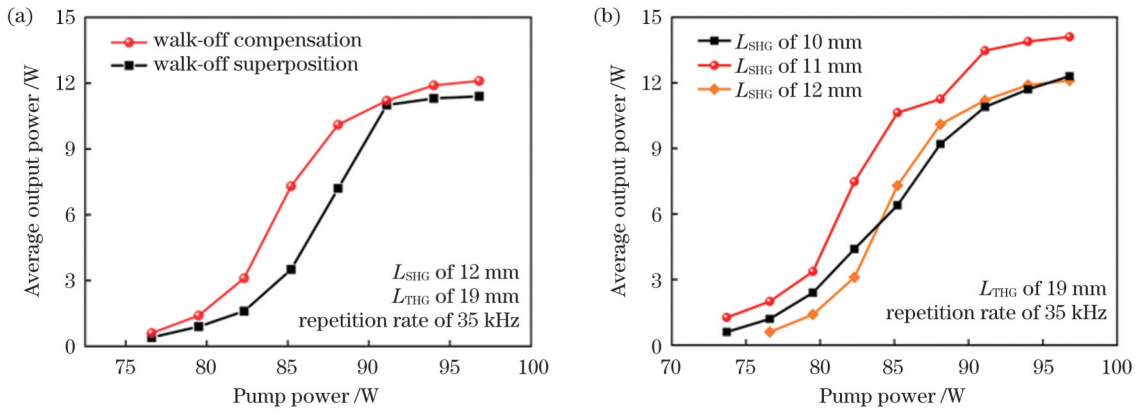

图 3　355 nm 紫外光输出功率随泵浦光功率的变化曲线。(a)不同走离情况下；(b)不同 SHG 晶体长度下

Fig. 3　Output power of 355 nm UV laser versus pump power. (a) Under different walk-off conditions; (b) under different SHG crystal lengths

高(14.1 W),而当二倍频晶体长度为 10 mm 和 12 mm 时得到的 355 nm 紫外光输出功率基本一致,分别为 12.3 W 和 12.1 W。同时,测量了二倍频晶体在三种长度下的 532 nm 绿光输出功率随泵浦光功率的变化,如图 4 所示。可知:当二倍频晶体长度发生变化时,最大泵浦功率处的 532 nm 绿光输出功率几乎一致,分别为 24.3、25.2 和 24.9 W;而当二倍频晶体长度为 11 mm 时,最大泵浦功率处的 355 nm 紫外激光输出功率与其他两晶体长度时的相差近 2 W。由此证明,当二倍频晶体长度为 11 mm 时实现了最大功率 355 nm 紫外激光输出,这是由于实现了最佳走离补偿。

同时,我们也知道,晶体的走离效应通常会严重影响产生的激光的光束质量。因此,在实验过程中,我们同时监视了走离效应对产生的 355 nm 紫外激光的光束质量的影响。当 355 nm 紫外激光平均输出功率最高时,使用光束质量分析仪分别在走离补偿和走离叠加两种情况下对 355 nm 紫外激光横向和纵向的光束质量进行测量,测量结果如图 5 所示。可以看出:在走离叠加情况下,获得的 355 nm 紫外光的 M_x^2 和 M_y^2 分别为 1.15 和 1.23;在走离补偿情况下,获得的 355 nm 紫外光的 M_x^2 和 M_y^2 分别为 1.13 和 1.18。可以看出,走离补偿可以很好地改善获得的 355 nm 紫外激光的光束质量。

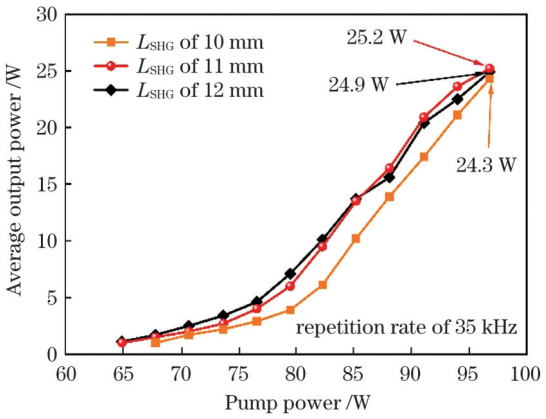

图 4　不同 SHG 晶体长度下 532 nm 绿光输出功率随泵浦光功率的变化曲线

Fig. 4　Output power of 532 nm green laser versus pump power under different SHG crystal lengths

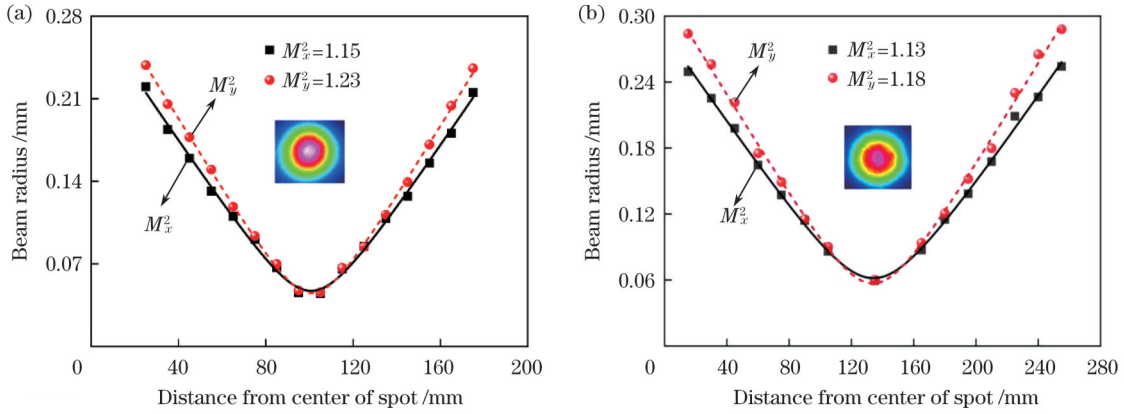

图 5　355 nm 紫外光的光束质量。(a)走离叠加情况下;(b)走离补偿情况下

Fig. 5　Beam quality of 355 nm UV laser. (a) Under walk-off superposition condition; (b) under walk-off compensation condition

最终确定腔内二倍频与三倍频晶体按图 2(b)所示的光轴方向放置。在走离补偿情况下,当泵浦注入功率为 96.8 W 时,不同重复频率下的 355 nm 激光输出功率曲线如图 6 所示。可以看出:当重复频率为 35 kHz 时,355 nm 紫外光输出功率达到最高(14.1 W),并且随着重复频率的降低而逐渐增加;随着泵浦功率的增加,355 nm 紫外光输出功率的增加越来越平缓,这是因为随着泵浦注入功率的增加,激光器系统中的热量和非辐射损耗会逐渐增加,所以输出功率的增长速率降低。尤其是在高泵浦功率注入下,系统会达到一个饱和点,即使进一步提高泵浦注入功率,输出功率也不会显著增加。当 355 nm 紫外光平均输出功率为 14.1 W 时,使用快速光电探测器测得 355 nm 紫外光的脉冲宽度为 12.8 ns,如图 7(a)所示。同时使用功率计测量 355 nm 紫外光在 10 h 内的功率稳定性,结果如图 7(b)所示,功率稳定性(均方根)优于 0.9%。

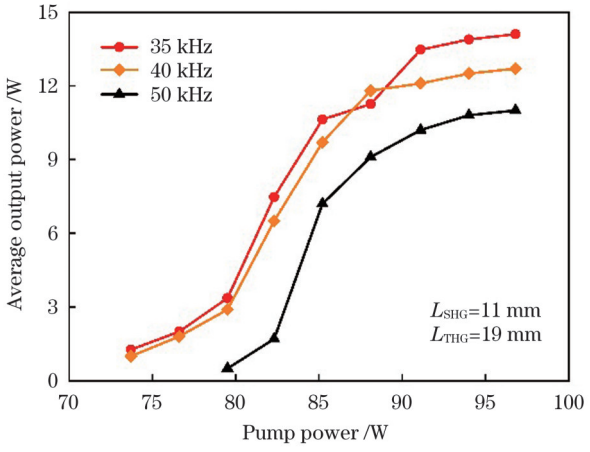

图 6　不同重复频率下 355 nm 紫外光输出功率随泵浦光功率的变化曲线

Fig. 6　Output power of 355 nm UV laser versus pump power under different repetition frequencies

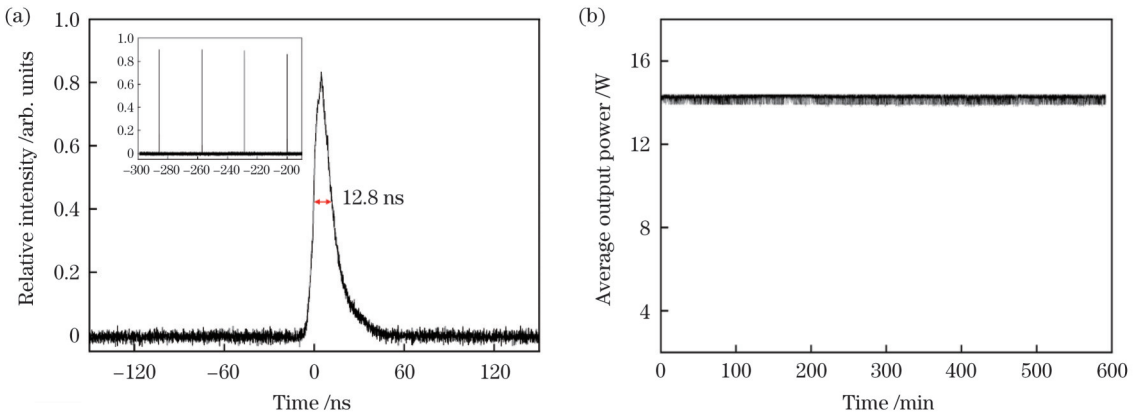

图 7 最大平均功率输出时的波形和功率稳定性。(a) 355 nm 紫外光脉冲波形;(b) 355 nm 紫外光功率稳定性

Fig. 7 Waveform and power stability at maximum average power output. (a) 355 nm UV laser pulse waveform; (b) 355 nm UV laser power stability

4 结 论

在腔内放置两块 LBO 晶体分别进行二倍频转换和三倍频转换,制备了一台高功率全固态内腔三倍频 355 nm 紫外激光器。利用两块非线性晶体之间的走离补偿技术,提高了 355 nm 紫外光的输出功率并且改善了光束质量。同时,大幅度放大了三倍频晶体处基频光的光斑半径,有效地提高了晶体的使用寿命。最终实现了高功率、高光束质量、高稳定的 355 nm 紫外光输出。当泵浦注入功率为 96.8 W 时得到了 14.1 W 的 355 nm 紫外光输出,相应的红外光到紫外光的光-光转换效率为 33.7%,脉冲宽度为 12.8 ns,脉冲重复频率为 35 kHz,光束质量因子优于 1.18。当平均输出功率为 14.1 W 时,355 nm 紫外光在 10 h 内的功率稳定性优于 0.9%。该激光器具有系统结构简单、平均功率高、光束质量好等优点,为其他同样采用双端垂直切面的 LBO 晶体进行三倍频转换的研究提供了重要的参考价值。同时这些优点使得该激光器适用于发光二极管、液晶显示屏、陶瓷和玻璃切割等领域。

参 考 文 献

[1] Wu Y C, Chang F, Fu P Z, et al. High-average-power third harmonic generation at 355 nm with CsB_3O_5 crystal[J]. Chinese Physics Letters, 2005, 22(6): 1426-1428.

[2] 陈志城, 刘文鑫, 吕风洋, 等. 355 nm 皮秒激光对柔性电路板盲孔加工的研究[J]. 应用激光, 2022, 42(5): 58-65.
Chen Z C, Liu W X, Lü F Y, et al. Research on blind hole machining of flexible circuit board by 355 nm picosecond laser[J]. Applied Laser, 2022, 42(5): 58-65.

[3] Li X D, Wu W T, Yan R P, et al. 10 kHz, 10 ns, 13.4 mJ Nd: YAG based frequency-tripled burst-mode MOPA source at 355 nm [J]. Optics & Laser Technology, 2019, 114: 190-195.

[4] Wang C X, Wang G Y, Hicks A V, et al. High-power *Q*-switched TEM_{00} mode diode-pumped solid state lasers with >30 W output power at 355 nm[J]. Proceedings of SPIE, 2006, 6100: 610019.

[5] Wei J, Jin P X, Cao X C, et al. Dircct generation of a stable multi-beam pulsed 355 nm UV laser based on a micro-lens array[J]. Chinese Optics Letters, 2022, 20(4): 041405.

[6] Yan X, Liu Q, Chen H, et al. 35.1 W all-solid-state 355 nm ultraviolet laser[J]. Laser Physics Letters, 2010, 7(8): 563-568.

[7] Chen H, Liu Q, Yan P, et al. High-power 355 nm ultraviolet lasers operating at ultrahigh repetition rate[J]. Laser Physics Letters, 2013, 10(2): 025401.

[8] Yan X P, Liu Q, Gong M, et al. Over 8 W high peak power UV laser with a high power *Q*-switched Nd: YVO_4 oscillator and the compact extra-cavity sum-frequency mixing[J]. Laser Physics Letters, 2009, 6(2): 93-97.

[9] Yang H W, Li D Z, Wang B, et al. End-pump high efficiency 355 nm laser with a convex - concave cavity and optically-uncoated Brewster angle-cut LiB_3O_5 crystal[J]. Journal of Optics, 2019, 21 (11): 115501.

[10] Xu S, Zhai S Y, Li B X, et al. High power and conversion efficiency intracavity ultraviolet laser at 355 nm[J]. Infrared Physics & Technology, 2023, 128: 104485.

[11] 王海龙, 杨慧琦, 苏静, 等. 基于单共振光学参量振荡器实现近红外到中红外激光输出的实验研究[J]. 中国激光, 2022, 49(18): 1801005.
Wang H L, Yang H Q, Su J, et al. Experimental study of near-infrared to mid-infrared laser output based on single resonant optical parametric oscillator[J]. Chinese Journal of Lasers, 2022, 49(18): 1801005.

[12] 赵志斌, 陈浩, 徐东昕, 等. LD端面抽运全固态声光调 *Q* 228.5 nm 深紫外激光器[J]. 中国激光, 2022, 49(3): 0315001.
Zhao Z B, Chen H, Xu D X, et al. LD end-pumped all-solid-state acousto-optical *Q*-switched 228.5 nm deep ultraviolet laser[J]. Chinese Journal of Lasers, 2022, 49(3): 0315001.

[13] 陈忆兰, 刘继桥, 王明建, 等. 310 nm 紫外固体拉曼激光器[J]. 中国激光, 2023, 50(22): 2201005.
Chen Y L, Liu J Q, Wang M J, et al. 310 nm ultraviolet solid-state Raman laser[J]. Chinese Journal of Lasers, 2023, 50(22): 2201005.

[14] 侯杰, 贾海旭, 白雅苏拉. 915 nm激光二极管端面泵浦的高稳定性全固态 355 nm 紫外激光器[J]. 激光与光电子学进展, 2021, 58 (19): 1914003.
Hou J, Jia H X, Bai Y. 355 nm all-solid state ultraviolet laser with high stability end-pumped by 915 nm laser diode[J]. Laser & Optoelectronics Progress, 2021, 58(19): 1914003.

[15] 王金艳, 李世杰, 刘天红, 等. 全固态 289.9 nm 紫外激光器的研究[J]. 中国激光, 2022, 49(7): 0701001.
Wang J Y, Li S J, Liu T H, et al. Research on all solid-state ultraviolet laser at 289.9 nm[J]. Chinese Journal of Lasers, 2022, 49(7): 0701001.

[16] 程梦尧, 王兆华, 何会军, 等. 高效率三倍频产生 355 nm 皮秒激光的实验研究[J]. 物理学报, 2019, 68(12): 124205.
Cheng M Y, Wang Z H, He H J, et al. Efficient third harmonic

generation of 355 nm picosecond laser pulse[J]. Acta Physica Sinica, 2019, 68(12): 124205.
[17] Yan X P, Liu Q, Pei C, et al. High-power 355 nm third-harmonic generation with effective walk-off compensation of LBO[J]. Journal of Optics, 2014, 16(4): 045201.
[18] Jung C, Shin W, Yu B A, et al. Enhanced 355-nm generation using a simple method to compensate for walk-off loss[J]. Optics Express, 2012, 20(2): 941-948.
[19] Boyd G D, Kleinman D A. Parametric interaction of focused Gaussian light beams[J]. Journal of Applied Physics, 1968, 39(8): 3597-3639.
[20] 姚建铨. 非线性光学频率变换及激光调谐技术[M]. 北京: 科学出版社, 1995.
Yao J Q. Nonlinear optical frequency conversion and its laser frequency modulation technology[M]. Beijing: Science Press, 1995.
[21] 蔡添志, 许惠英, 王晓忠, 等. LBO的腔内倍频特性研究[J]. 红外与激光工程, 2007, 36(S1): 71-74.
Cai T Z, Xu H Y, Wang X Z, et al. Intracavity frequency-doubling characterization of LBO[J]. Infrared and Laser Engineering, 2007, 36(S1): 71-74.
[22] 薛建华, 任清华, 王爱坤. LBO晶体II类相位匹配走离角及互作用长度的计算[J]. 人工晶体学报, 2009, 38(6): 1463-1466, 1471.
Xue J H, Ren Q H, Wang A K. Calculation of type II phase-matching walk-off angle and interaction length of LBO crystals[J]. Journal of Synthetic Crystals, 2009, 38(6): 1463-1466, 1471.
[23] 宗妍. LD侧面泵浦电光调Q绿光及紫外脉冲激光器的研究[D]. 西安: 西北大学, 2008.
Zong Y. Study on LD side-pumped electro-optic Q-switched green and ultraviolet pulse Laser[D]. Xi'an: Northwest University, 2008.
[24] 高锋, 蔡云鹏, 白振旭, 等. 非线性晶体走离效应下的二倍频效率研究[J]. 红外与激光工程, 2023, 52(8): 20230254.
Gao F, Cai Y P, Bai Z X, et al. SHG efficiency of nonlinear crystal walk-off effect[J]. Infrared and Laser Engineering, 2023, 52(8): 20230254.

High-Power, High-Beam-Quality, All-Solid-State Intracavity Frequency Tripling 355 nm Laser

Liu Xinyu[1], Zhang YanLin[1], Cao Xuechen[1], Yang Jie[1], Su Jing[1,2], Lu Huadong[1,2*]

[1]*State Key Laboratory of Quantum Optics and Quantum Optics Devices, Institute of Opto-Electronics, Shanxi University, Taiyuan* 030006, *Shanxi, China*;

[2]*Collaborative Innovation Center for Extreme Optics, Shanxi University, Taiyuan* 030006, *Shanxi, China*

Abstract

Objective High-power, high-beam-quality, all-solid-state 355 nm ultraviolet lasers, with their short wavelengths, easy focusability, and high energy characteristics, are being widely applied in precision machining, biomedical, optical manufacturing, and optical sensing fields. The most common technique by which to achieve 355 nm ultraviolet output is the use of a master oscillator power amplifier (MOPA) to amplify 1064 nm seed light through single or multiple stages. This is followed by triple-frequency conversion outside the cavity. However, the overall complexity of the system is not conducive to the design of high-stability ultraviolet lasers. Compared to external frequency tripling technology, the intracavity frequency tripling process can fully utilize the high power density inside the cavity for nonlinear mixing, thereby improving the conversion efficiency, and its compact overall structure and high stability make it an effective means by which to realize the widespread application of high-power all-solid-state 355 nm ultraviolet lasers. To further improve the output power of the 355 nm ultraviolet laser achieved by intracavity frequency conversion technology and to reduce the beam quality factor to a value below 1.2, this study first examines the impact of walk-off on the output power of 355 nm lasers under the same and different optical axis orientations of two nonlinear crystals. Then, walk-off compensation technology between nonlinear crystals is used to effectively compensate for the walk-off phenomenon caused by the mixing of fundamental frequency light and harmonic light in the triple-frequency crystal, thereby increasing the output power of the 355 nm laser to 14.1 W.

Methods To obtain a high-power, high-beam-quality, all-solid-state 355 nm ultraviolet laser, a solid-state intracavity Nd∶YVO_4 laser is first designed and manufactured to significantly enlarge the spot radius of the fundamental frequency light at the tripling crystal while ensuring high power output, thereby extending the lifespan of the nonlinear crystal. Then, the second harmonic generated by the type I phase-matching nonlinear lithium triborate (LBO) crystal, has a polarization state perpendicular to that of the fundamental frequency light. The incident fundamental light and the generated second harmonic perfectly satisfy the type II phase-matching conditions of the triple-frequency LBO crystal, achieving the output of a triple-frequency 355 nm laser. On this basis, by comparing the output power of a 355 nm laser with different lengths of the second harmonic crystal, the optimal triple-frequency conversion efficiency is achieved. The study also explores the differences in 532 nm laser output power and beam quality of 355 nm laser under different lengths of the second harmonic crystal and the conditions of the same and different optical axis directions of two nonlinear crystals.

Results and Discussions First, frequency conversion is achieved using LBO crystals with 19 mm and 11 mm in length, and the differences in the output power of a 355 nm laser under the same and different optical axis orientations of the two nonlinear crystals are recorded. When walk-off is compensated, the output power of the 355 nm laser reaches 14.1 W, which is 2 W higher than that observed before the walk-off is increased [Fig. 3(a)]. By adjusting the lengths of the different second harmonic crystals, the optimal triple-frequency conversion efficiency is achieved [Fig. 3(b)], indicating that the triple-frequency conversion efficiency is the best when the second harmonic crystal length is 11 mm. The transformation relationship of the 532 nm laser output power with the pump light power is also measured under different lengths of the second harmonic crystal (Fig. 4), similarly indicating that the second harmonic conversion efficiency is the highest under the same second harmonic crystal. Based on this, the differences in the beam quality of the 355 nm laser under compensated and uncompensated walk-off conditions are measured [Fig. 5(a) and Fig. 5(b)], showing that walk-off compensation technology effectively compensates for the walk-off phenomenon caused by the mixing of fundamental frequency light and harmonic light in the triple-frequency crystal, thereby improving both the triple-frequency conversion efficiency and beam quality. At the highest average 35 nm laser output power, the corresponding pulse width is 12.8 ns [Fig. 7(a)], and the beam quality is better than 1.18 (Fig. 5). The power stability (root mean square) at 14.1 W for 10 h is better than 0.9% [Fig. 7(b)].

Conclusions In summary, this study describes the creation of a high-power, all-solid-state 355 nm ultraviolet laser by placing two LBO crystals inside a cavity for second harmonic generation (SHG) and third harmonic generation (THG), respectively. The walk-off compensation technique between the two nonlinear crystals inside the cavity structure is experimentally verified to enhance the output power and improve the beam quality of the 355 nm laser. This ensures that even when the fundamental frequency spot diameter at the triple-frequency crystal reaches 836 μm, the 355 nm laser can still achieve high power, high beam quality, and highly stable output. An output of 14.1 W for 355 nm pulsed light is obtained with a pump injection power of 96.8 W, corresponding to an infrared-to-ultraviolet light-to-light conversion efficiency of 32.1%, a pulse width of 12.8 ns, a pulse repetition frequency of 35 kHz, and a beam quality of better than 1.18. The power stability (root mean square) at 14.1 W over 10 h is better than 0.9%. The design proposed in this study features a simple system structure, high average power, and good beam quality. It also suggests that for other research using LBO crystals with double-ended vertical cross-sections for tripling frequency, adopting this design will yield higher 355 nm laser output power and conversion efficiency. These characteristics make the laser suitable for widespread commercial applications in fields such as light-emitting diode, liquid crystal display, ceramics, and glass cutting.

Key words 355 nm UV laser; intracavity frequency tripling; walk-off compensation; high power; all-solid-state